Materials Research Bulletin 65 (2015) 175–182

Contents lists available at ScienceDirect

Materials Research Bulletin

journal homepage: www.elsevier.com/locate/matresbu

Anisotropic magnetoresistance in facing-target reactively sputtered epitaxial γ'-Fe_4N films

Z.R. Li [a], X.P. Feng [a], X.C. Wang [b], W.B. Mi [a,*]

[a] Tianjin Key Laboratory of Low Dimensional Materials Physics and Preparation Technology, Faculty of Science, Tianjin University, Tianjin 300072, China
[b] Tianjin Key Laboratory of Film Electronic & Communicate Devices, School of Electronics Information Engineering, Tianjin University of Technology, Tianjin 300384, China

ARTICLE INFO

Article history:
Received 11 October 2014
Received in revised form 19 January 2015
Accepted 26 January 2015
Available online 28 January 2015

Keywords:
A. Magnetic materials
A. Nitrides
B. Epitaxial growth
D. Electrical properties

ABSTRACT

The negative anisotropic magnetoresistance that comes from the spin-down conduction electrons are observed in facing-target sputtered epitaxial γ'-Fe_4N films with different film thicknesses, substrates and orientations. Anisotropic magnetoresistance of γ'-Fe_4N films on $LaAlO_3$(1 0 0) is larger than other substrates. The magnitude of anisotropic magnetoresistance in (1 0 0)-oriented films is always larger than (1 1 0)-oriented films. The anisotropic magnetoresistance is intimately related to the magnetocrystalline anisotropy. Fourier coefficient $C_{2\theta}$ and $C_{4\theta}$ of $\cos 2\theta$ and $\cos 4\theta$ terms strongly depend on the measuring temperature. No significant influence of magnetic field on $C_{2\theta}$ and $C_{4\theta}$ appears. The marked change of $C_{2\theta}$ and appearance of $C_{4\theta}$ at low temperatures are from crystal field splitting of d orbitals induced by the lattice change due to the tensile stress from substrate and the compressive stress from decreased temperatures.

A. Magnetic materials; A. Nitrides; B. Epitaxial growth; D. Electrical properties

1. Introduction

Ferromagnetic iron nitrides have attracted much attention for spintronic devices due to their excellent magnetic properties. Among them, γ'-Fe_4N was theoretically predicted to have a negative spin polarization of −100% [1]. The high spin polarization was experimentally determined by point-contact Andreev reflection and spin-resolved photoelectron spectroscopy [2,3]. The negative spin polarization was also confirmed via inverse tunnel magnetoresistance and inverse current-induced magnetization switching effect in magnetic tunnel junctions with a γ'-Fe_4N electrode [4–6]. Because of the negative spin polarization, γ'-Fe_4N films may show various special magnetotransport properties.

The anisotropic magnetoresistance (AMR) is one of the most fundamental characteristics involving magnetic and electronic transport properties, where the resistivity of the sample is dependent on the relative angle between the magnetization and applied current directions [7–20]. AMR effects have been studied in different ferromagnetic materials, such as Fe [17], Co [17], Ni [17], Fe_3O_4 [18–20], $La_{1-x}Ca_xMnO_3$ [21,22], $Ga_{1-x}Mn_xAs$ [23]. Generally, AMR ratio is defined as

$$\frac{\Delta\rho}{\rho} = \frac{\rho_{//} - \rho_{\perp}}{\rho_{\perp}} \quad (1)$$

where $\rho_{//}(\rho_{\perp})$ represents resistivity for the case of the current parallel (perpendicular) to the magnetization. The negative AMR was observed in the polycrystalline, pseudo-single-crystal and epitaxial γ'-Fe_4N films, and the negative AMR was considered to be clear evidence of spin-down conduction electron in γ'-Fe_4N films [24–28]. However, in the triode-sputtered epitaxial γ'-Fe_4N films deposited on $SrTiO_3$(0 0 1) substrates, the positive AMR was reported [29]. The sign of AMR is different from other reports and the origin of difference remains unclear. Recently, Kokado et al. theoretically analyzed the relationship between the AMR sign and s–d scattering process [30]. The result was drawn that the negative AMR ratio of γ'-Fe_4N was due to the dominant s–d scattering process of $s\downarrow \rightarrow d\downarrow$ [30]. In addition, the large stepwise change in the AMR ratio of γ'-Fe_4N appeared below 50 K [24,25]. The appearance of an anomalous $\cos 4\theta$ term and the enhancement of $\cos 2\theta$ term at low temperatures were also observed [25,27,28]. Crystal field effect was considered as the possible reason of these behaviors [27]. The reported AMR in the γ'-Fe_4N films presents different results. So, it is necessary to investigate the AMR in the γ'-Fe_4N films.

To clarify the physical origin, this work investigates the AMR effect in epitaxial γ'-Fe_4N films by changing film thickness, substrate and orientation. In the previous work, we have reported the surface morphology, microstructure, magnetic and electrical

* Corresponding author. Tel.: +86 22 27406991; fax: +86 22 27403425.
E-mail address: miwenbo@tju.edu.cn (W.B. Mi).

http://dx.doi.org/10.1016/j.materresbull.2015.01.053
0025-5408/

transport properties of epitaxial γ'-Fe_4N films with different thicknesses on various substrates [31]. In this paper, the epitaxial γ'-Fe_4N films with different lattice orientations and film thicknesses are fabricated on different substrates by facing-target reactive sputtering. AMR effect of epitaxial γ'-Fe_4N films has been investigated in details.

2. Experimental details

Epitaxial γ'-Fe_4N films with different thicknesses were fabricated on MgO(1 0 0), $SrTiO_3$(1 0 0), $SrTiO_3$(1 1 0) and $LaAlO_3$ (1 0 0) substrates by a DC reactive facing-target sputtering method. MgO(1 0 0), $SrTiO_3$(1 0 0), $SrTiO_3$(1 1 0) and $LaAlO_3$(1 0 0) substrates were defined as MgO(1 0 0), STO(1 0 0), STO(1 1 0) and LAO(1 0 0), respectively. Details for the epitaxial growth of γ'-Fe_4N were referred to our previous work [31]. For comparison, the polycrystalline γ'-Fe_4N films were also grown on glass substrate. The film thickness was determined using a Dektak 6M surface profiler, and confirmed by transmission electron microscopy (TEM). The structure was analyzed by X-ray diffraction (XRD) with Cu Ka radiation (wavelength 1.5406 Å) and high-resolution TEM (HRTEM). The AMR effect was measured with a standard four-terminal method by a Quantum Design physical property measurement system (PPMS-9) at temperatures ranging from 5 to 300 K. The applied magnetic field was parallel to the film plane. At 5 and 300 K, different magnetic fields from 0.2 to 50 kOe were applied for AMR measurements. At other selected temperatures, a 10-kOe field was applied.

3. Results and discussion

Fig. 1a shows the XRD θ–2θ pattern of epitaxial γ'-Fe_4N films on MgO(1 0 0). Except for the diffraction peaks from face-centered cubic MgO(2 0 0) and (4 0 0), only peaks from γ'-Fe_4N(1 0 0) and (2 0 0) that located at 23.3° and 47.9° appear. No other peaks from γ'-Fe_4N can be observed, suggesting that the film grows with a preferred (1 0 0) orientation. Fig. 1d gives the XRD θ–2θ pattern of epitaxial γ'-Fe_4N films on STO(1 1 0). Only a peak at 70.1° from γ'-Fe_4N(2 2 0) is observed, showing the film grows with a preferred (1 1 0) orientation. The preferred orientation can not completely account for the epitaxial growth of the films. In general, ϕ scan and pole figure are used to characterize the epitaxial structure by identifying the symmetry of a diffraction peak. For confirming the preferred oriented films are epitaxial, X-ray ϕ scan is performed. X-ray is collected at $2\theta = 41.22°$, where no peaks from MgO and STO substrates appear, and only a peak from γ'-Fe_4N(1 1 1) is detected. Fig. 1b and e shows the X-ray ϕ scan of epitaxial γ'-Fe_4N films on MgO(1 0 0) and STO(1 1 0). For γ'-Fe_4N films on MgO(1 0 0), sharp 4-fold symmetric diffraction peaks of γ'-Fe_4N(1 1 1) with identical intervals appear. According to XRD results, the epitaxial relationship of γ'-Fe_4N films on MgO(1 0 0) can be confirmed as γ'-Fe_4N (1 0 0) [0 0 1]|| MgO(1 0 0) [0 0 1]. For γ'-Fe_4N films on STO(110), 2-fold symmetric peaks with identical intervals appear, suggesting that epitaxial relationship of γ'-Fe_4N films on STO(1 1 0) is γ'-Fe_4N (1 1 0) [1 1 0]|| STO(1 1 0) [1 1 0]. The above X-ray θ–2θ and ϕ scan suggest that the γ'-Fe_4N films on MgO(1 0 0) and STO(1 1 0) are epitaxial and cubic. Fig. 1c and f gives the X-ray pole figures of the γ'-Fe_4N films on MgO(1 0 0) and STO(1 1 0), showing cubic structure and in-plane rotational symmetry of γ'-Fe_4N films. On the (1 1 1) plane, the (1 0 0)-oriented films have four symmetrical diffraction peaks, while (1 1 0)-oriented films show two symmetrical diffraction peaks. These relevant strong diffraction peaks further suggest that all the films are fully epitaxial.

Fig. 2 shows the cross-sectional HRTEM images of epitaxial γ'-Fe_4N films on MgO(1 0 0) and STO(1 1 0). In Fig. 2a, the HRTEM image at γ'-Fe_4N/MgO(1 0 0) interface shows the epitaxial growth of the film even though the lattice mismatch rate is 10%, which further confirms the X-ray θ–2θ, ϕ scan and pole figures results.

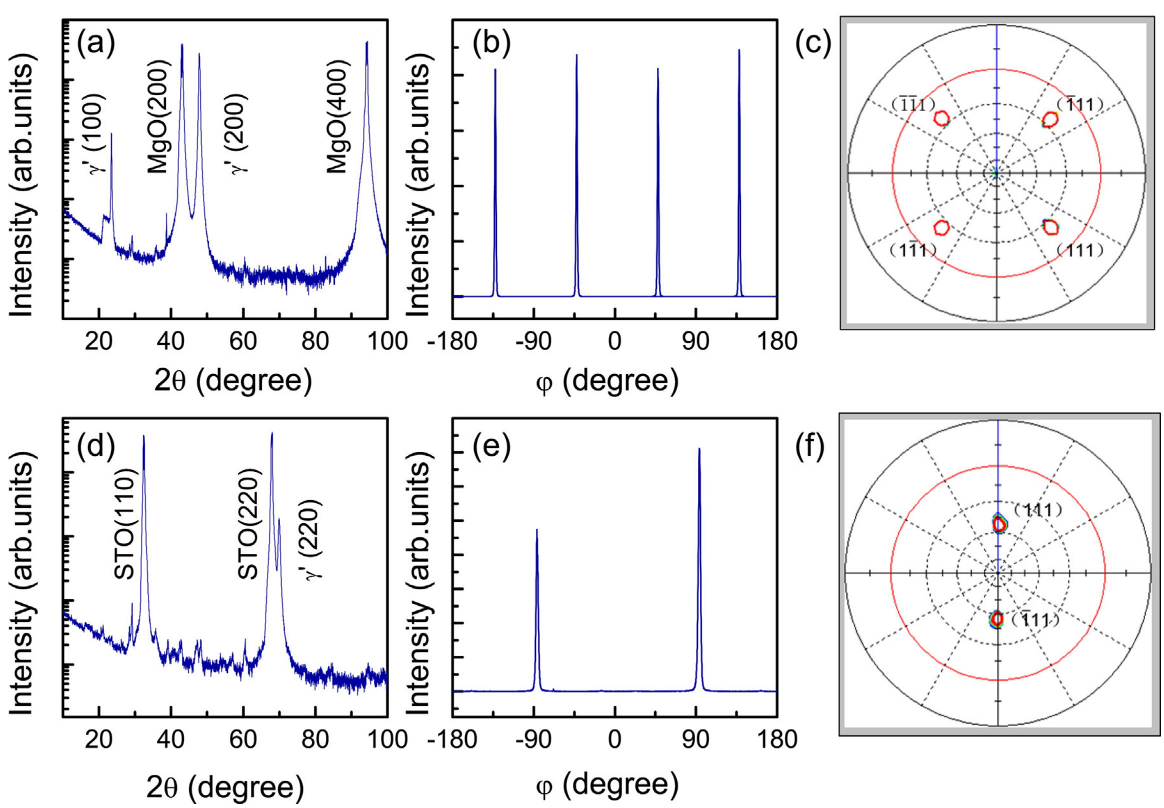

Fig. 1. X-ray θ–2θ,ϕ scan and pole figure of epitaxial γ'-Fe_4N films on (a)–(c) MgO(1 0 0) and (d)–(f) STO(1 1 0) substrates.